

# HE-LHC FINAL FOCUS: FLAT BEAM PARAMETERS AND ENERGY DEPOSITION STUDIES \*

J. L. Abelleira, E. Cruz-Alaniz, L. van Riesen-Haupt, A. Seryi  
 John Adams Institute, University of Oxford, UK

## Abstract

The High Energy LHC (HE-LHC) project is studying the feasibility of a new proton-proton collider with a beam energy of 13.5 TeV. The nominal optics features a  $\beta^*$  of 0.25 m and crab-cavities. Here we present a flat-beam optics that can be used with a non-zero crossing angle, in the absence of crab cavities. This is followed by energy deposition studies for the superconducting quadrupoles and dipole separators. The total dose in these magnets coming from the collision debris is evaluated.

## THE HIGH ENERGY LHC

The High Energy LHC (HE-LHC) aims at providing  $pp$  collisions at a center of mass energy of 27 TeV, making use of the existing LHC tunnel [1]. A large beam rigidity is imposed by the circulating 13.5-TeV beams in the 26.7-km LHC tunnel, and requires the installation of 16-T bending dipoles. To this purpose, the same magnet technology as for the FCC-hh magnets can be applied [2].

## FINAL FOCUS DESIGN

Two high luminosity Interaction Regions (IR) are envisaged at IR1 & IR5. An identical triplet at each side of both IRs focalizes the beams at collision to maximize the luminosity. The design of this triplet is discussed in [3]. This final focus system is compatible with a round and a flat optics. The main parameters of the final focus quadrupoles, identical for all of them, are shown in Table 1. The transverse cross section of the FLUKA model for the magnets is shown in Fig. 1.

Table 1: Quadrupole Parameters of the Final Focus Triplet

Parameter	Value
Gradient	146 T/m
Inner radius	44.6 mm
Absorber thickness	20 mm
Inner coil radius	70.4 mm

The quadrupoles differ in length only, as seen in Fig. 2. Q2 consists of two units, and its gradient has opposite sign to Q1 and Q3. The main parameters of the options discussed in this paper are shown in Table 2.

\* Work supported by EuroCircol, EU's Horizon 2020 grant No 654305 & STFC grant to the John Adams Institute.

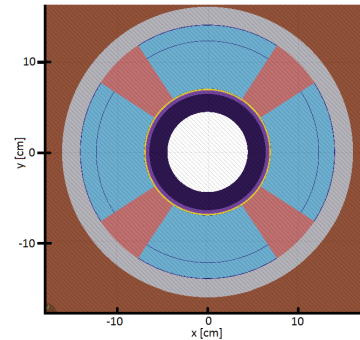


Figure 1: Transverse cross section of the FLUKA model for the triplet quadrupoles, including the tungsten shielding.

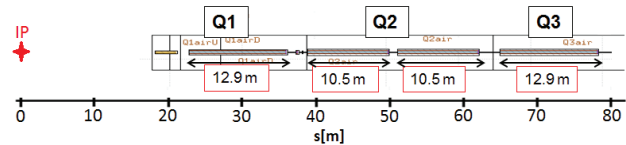


Figure 2: Schematic of the final-focus triplet.

## FLAT BEAM OPTICS

The use of flat beams has been studied for the FCC-hh as an alternative to the use of crab cavities [4]. Flat beams restore some of the luminosity lost with the crossing angle in the absence of crab cavities. This is achieved by reducing  $\beta_y^*$  while the Piwinski angle ( $\phi$ ) is decreased through an enlarged  $\beta_x^*$ , as  $\phi = \theta \sigma_s / 2 \sqrt{\epsilon \beta_x^*}$ , where  $\theta$  is the full crossing angle,  $\sigma_s$  is the longitudinal beam size, and  $\epsilon$  is the transverse beam emittance. If the beam separation ( $\Delta_{in}$ ) is kept, the crossing angle can be reduced too, as  $\theta = \Delta_{in} \sqrt{\epsilon / \beta_x^*}$ . However, the beam separation must be enlarged as the flat beam ratio ( $\beta_x^* / \beta_y^*$ ) increases [5]. This causes that part of the benefit of flattening the beam is diluted if the beam separation is increased. Thus, the performance of the flat beam optics depends heavily on the beam separation.

We have explored a range of parameters to define an optimum set of  $\{\beta_x^*, \beta_y^*\}$  for the flat option. We have looked at maximizing the integrated luminosity without incurring in a large flat beam ratio, while keeping the total beam-beam parameter below 0.02 and the nominal luminosity below  $30 \cdot 10^{34} \text{ cm}^{-2} \text{ s}^{-1}$  [6]. With these constraints, an optimum working point for the flat optics was found at  $\beta_x^* = 0.4 \text{ m}$ ,  $\beta_y^* = 0.1 \text{ m}$ . In the worst case of having to increase the beam separation by 50 %, the luminosity loss with respect to the round optics with crab cavities would be 16 %. On the other hand, the luminosity loss of running the round optics without crab cavities would be as large as 32 %.

Table 2: HE-LHC parameter comparison of the different optics choices in this paper, round and flat. For the flat beam option, two different beam separations are considered

	nominal	flat
Bunch population, $N$ [ $\cdot 10^{11}$ ]		2.2
Normalized emittance, $\epsilon_N$ [ $\mu\text{m}$ ]		2.5
Number of bunches, $n_b$		2808
Bunch length, $\sigma_s$ [cm]		7.55
$\beta_x^*$ [m]	0.25	0.4
$\beta_y^*$ [m]	0.25	0.1
Beam separation, $\Delta_{in}$ [ $\sigma$ ]	10	10/15
Full crossing angle, $\theta$ [ $\mu\text{rad}$ ]	260	208/312
Crab cavities	yes	no
Piwinski angle, $\phi$	1.5	0.94/1.41
Total tune shift $\xi_t$ [ $\cdot 10^{-3}$ ]	20	16/11
Nominal luminosity, $L$ [ $\cdot 10^{34} \text{ cm}^{-2} \text{ s}^{-1}$ ]	26	25/20
Average luminosity, $L_{ave}$ [ $\text{fb}^{-1}/\text{day}$ ]	6.2	5.8/5.2

Figure 3 shows the luminosity performance of the different optics, until their respective optimum run time. The optimum run times are in the range from 3 to 4.1 h, assuming a preparation time between runs of 3 h. The luminosity decays due to the particle burn out, which is faster than the emittance damping time (3.6 h). For this reason, unlike the FCC-hh, there is no increase in luminosity. We can see that the performance of the flat optics with  $\Delta_{in} = 10\sigma$  is almost identical than that for round beams with crab cavities. For  $\Delta_{in} = 15\sigma$ , on the other hand, the luminosity is considerably lower. However, it is still better than for the case with round beams and no crab cavities.

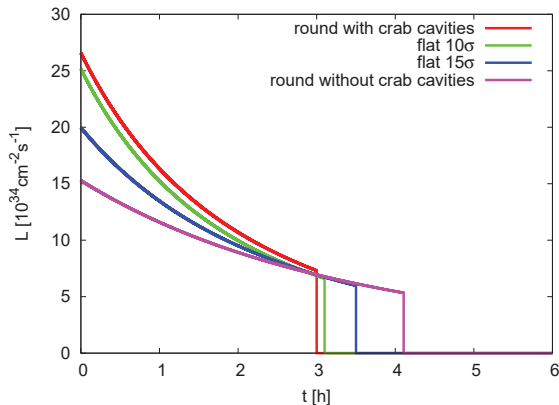


Figure 3: Luminosity evolution for the round and flat optics.

## INTERACTION REGION OPTICS

Figure 4 shows the betatron functions for the round optics, that present a maximum of 19 km. The corresponding beam stay clear (BSC) is  $>12\sigma$ . The IR was designed with an optimization code [7] including several iterations with energy deposition simulations. Other aspects of this triplet, including matching to the arc, dynamic aperture and injection optics are also discussed in [3].

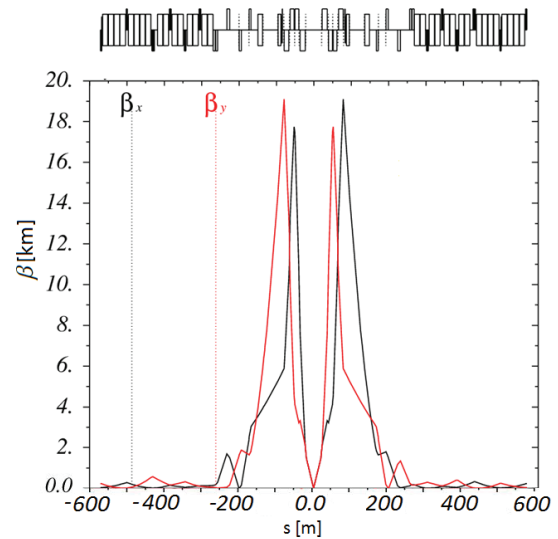


Figure 4: Interaction region for the round Optics ( $\beta^* = 0.25$  m).

## ENERGY DEPOSITION SIMULATIONS

The debris from the  $pp$  collisions has been simulated with FLUKA [8,9] in order to guarantee the triplet survival during the entire lifetime, estimated in  $10 \text{ ab}^{-1}$ . Energy deposition simulations are shown in Fig. 5 for the round optics. Two cases are presented, with beam crossing in the horizontal and vertical plane, respectively. The radiation profile is symmetric on both sides of the interaction point. This is because the quadrupole is also symmetric from the reference system of the debris particles. The differences between the two crossing planes are caused by the quadrupolar field of the triplet magnets, which changes from focalizing to defocalizing for the horizontal and for the vertical plane. The vertical crossing presents higher peak doses, which can be explained as Q1 and Q3 are defocalizing for this plane while Q2 is focalizing.

Content from this work may be used under the terms of the CC BY 3.0 licence © (2018). Any distribution of this work must maintain attribution to the author(s), title of the work, publisher, and DOI.

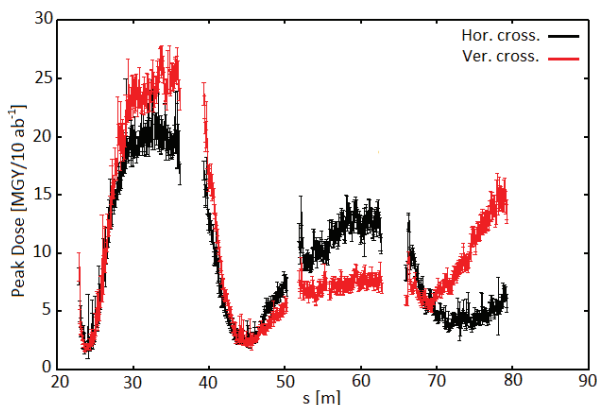


Figure 5: Peak dose profile for the round optics ( $\theta = 260$  mrad).

The maximum dose is found at Q1, and is lower than 30 MGy, which is considered the present limit for the magnet survival. In addition, the dose can be reduced if alternate crossing is applied, as for each crossing plane, the peak is found in a different location of the coil. This effect has been discussed for the FCC-hh final-focus [4, 10, 11]. The flat beam scenario has also been simulated, without any significant difference in peak dose, in spite of the smaller crossing angle. Not only the quadrupoles are shielded, but the beam pipe between magnets must be shielded too, otherwise a large peak dose would appear at the begging of each magnet. However, for technical reasons, not all the space between magnets can be shielded. Some space must be allocated for the interconnects. In this study we have assumed interconnects of 50 cm. If we assume instead 100-cm interconnects, we observe peaks at the beginning of both Q2 units [12].

Besides the peak dose, a very important aspect of to look at is the peak power density absorbed on the magnet coils. An excessive power produces a temperature increase that can induce a magnet quench. This limit is considered to be within the range 3-5 mW/cm<sup>3</sup> [13]. The peak power density is shown in Fig. 6. The power density is below 3 mW/cm<sup>3</sup>, which indicates that the triplet is well quench protected.

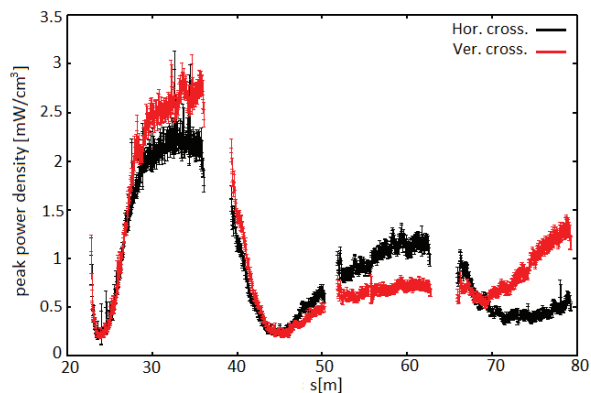


Figure 6: Peak power density for the round optics ( $\theta = 260$  mrad).

## DOSE IN DIPOLE SEPARATION D1

First studies have been carried out to estimate the dose in the first dipole separator, D1. This separation magnet has a length of 8 m and a magnetic field strength of 11.1 T. We have assumed coil aperture of 70 mm (radius), with a shielding of 5 mm, which gives a BSC > 30 $\sigma$ . Figure 7 shows the radiation profile in D1 for the horizontal and vertical crossing. Peak dose is almost 100 MGy, considerably larger than the limit. From these results we can conclude not only that D1 must be shielded, but that the thickness of the shielding must be more than 5 mm.

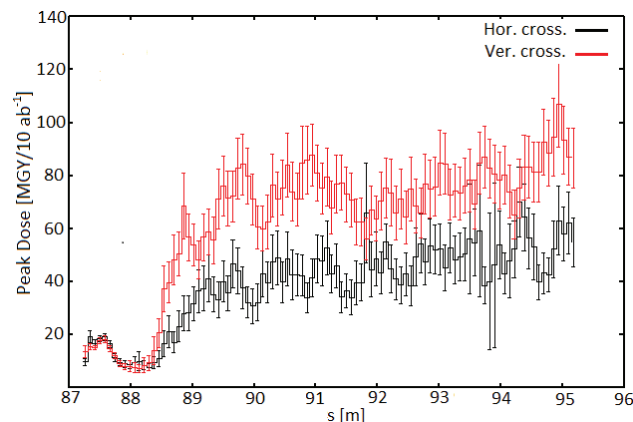


Figure 7: Peak dose profile for D1.

## CONCLUSIONS

We have presented a final focus system which has been optimized to minimize the energy deposition in the coils. We have also shown the option of a flat-beam optics, which is feasible with this triplet. We have found an optimum set of  $\beta_{x,y}^*$  that can be used in case crab cavities technology is not feasible for this machine. We have shown the strong dependence of the luminosity with the required beam separation. First radiation studies for separation dipoles have been performed, showing the need for shielding in D1, at least, in order to protect the superconducting coils. More work will be carried out to minimize the dose in D1, and to extend this study to the other separation/recombination dipole, D2.

## ACKNOWLEDGMENTS

We would like to acknowledge the collaboration with the rest of the HE-LHC group and to the CERN FLUKA team. In particular, we acknowledge Ilaria Besana for having built the FLUKA model of the FCC-hh quadrupole magnets, which was modified and re-scaled the HE-LHC magnets in this study.

## REFERENCES

- [1] D. Amorim *et al.*, “High-Energy LHC design”, presented at IPAC’18, Vancouver, Canada, April-May 2018, paper MOPMF064.
- [2] D. Shulte *et al.*, “Future Circular Collider Study”, FCC week 2018, Amsterdam, Netherlands, 2018.
- [3] L. van Riesen-Haupt *et al.*, “Experimental Interaction Region Optics for the High Energy LHC”, presented at IPAC’18, Vancouver, Canada, April-May 2018, paper MOPMK006.
- [4] J. L. Abelleira *et al.*, “Energy Deposition Studies and Luminosity Evolution for the Alternative FCC-hh Triplet”, presented at IPAC’18, Vancouver, Canada, April-May 2018, paper MOPMK003.
- [5] T. Pieloni *et al.*, “Beam Beam for the HE-LHC”, FCC Week 2018, Amsterdam, Netherlands, 2018.
- [6] J. L. Abelleira *et al.*, “HE-LHC with Flat beams”, FCC Week 2018, Amsterdam, Netherlands, 2018.
- [7] L. van Riesen-Haupt *et al.*, “A Code for Optimising Triplet Layout”, in *Proc. IPAC’17*, Copenhagen, Denmark, May 2017, paper TUPVA043, pp. 2163-2165.
- [8] A. Ferrari, P.R. Sala, A. Fassò, and J. Ranft, “FLUKA: a multiparticle transport code”, Rep. CERN-2005-10, INFN/TC05/11, SLAC-R-773, Oct. 2005.
- [9] G. Battistoni *et al.*, “Overview of the FLUKA code”, *Annals of Nuclear Energy*, vol. 82, pp. 10-18, Aug. 2015.
- [10] Roman Martin *et al.*, “Interaction region design driven by energy deposition”, *Physical Review Accelerators and Beams*, Volume 20, 2017.
- [11] F. Cerutti *et al.*, “Beam loss studies in IP”, FCC week 2018, Amsterdam, Netherlands, 2018.
- [12] J. L. Abelleira *et al.*, “IR1 & IR5 Radiation Shielding”, FCC Week 2018, Amsterdam, Netherlands, 2018.
- [13] Daniel Schoerling “Review of peak power limits for high luminosity IR triplet magnets”, FCC-hh other magnet design meeting, 23 June 2018.